GSA Data Repository Item 2019140

Napier, T.J., Hendy, I.L., Fahnestock, M.F., and Bryce, J.G., 2019, Provenance of detrital sediments in Santa Barbara Basin, California, USA: Changes in source contributions between the Last Glacial Maximum and Holocene: GSA Bulletin, https://doi.org/10.1130/B32035.1.

Data Repository

Bivariate correlation analysis of major elements

A Kendall's rank correlation was run to determine relationships between major elements. Significant positive relationships occur between Al and Fe, Al and Ti, Fe and Mg, and Fe and Ti ($p<0.01$; sample n=27, or n=26 for Ti correlations) (Figure DR1). Samples with individual elemental concentrations that exceeded the 2σ range of all samples were considered outliers and excluded from the correlation analysis for certain elements (see main text; e.g., L4 was excluded from Ti correlation).

K-means cluster analysis of catchment sample major element principal components and radiogenic isotopes

K-means cluster analysis was used to identify groups of samples within major element PC1 and PC2 space. Samples L3 and L30 were removed prior to clustering analysis, as these samples are outliers. To determine the appropriate number of sample groups, we applied the k-means cluster analysis using 2-6 groups, respectively, and assessed the silhouette values of each respective clustering result (Figure DR3). Higher silhouette values indicate a more appropriate clustering solution. The clustering result with four groups has the greatest number of samples with high silhouette values; for example, there are 11 samples with silhouette values over 0.7 (Figure DR3). Therefore, four groups is the most appropriate clustering solution for the catchment samples in PC1 and PC2 space, and was used in this study.

K-means cluster analysis was also used to determine the appropriate grouping of the Sr and Nd radiogenic isotope results. Catchment sample $^{87}Sr/^{86}Sr$ and $^{143}Nd/^{144}Nd$ were used for this analysis, and both were standardized prior to analysis. To determine the appropriate number of sample groups, we applied the k-means cluster analysis with group numbers of 2-6, respectively, and assessed the silhouette values of each respective clustering result (Figure DR4). The clustering result with five groups has the greatest number of samples with high silhouette values; for example, there are 21 samples with silhouette values over 0.4 (Figure DR4). Therefore, the most appropriate clustering solution for the catchment samples in Sr-Nd isotope space includes five groups, and this approach was used in this study.

Combined analysis of major element composition, $^{87}Sr/^{86}Sr$, ε_{Nd}, and predominant mineralogy

Isotopic measurements, major element composition, and mineralogy can all be used to characterize and discriminate sediment source areas. Principal component analysis (PCA) of the bed sediment samples' major element composition, $^{87}Sr/^{86}Sr$, ε_{Nd}, and predominant mineralogy enabled assessment of the influences on sample composition (Table DR6). All variables were standardized prior to PCA. The first principal component (PC1) has high positive loadings for plagioclase, ε_{Nd}, Al, Ti, and Fe, with strong negative loadings for $^{87}Sr/^{86}Sr$, K, quartz, and potassium feldspar. Thus, PC1 appears to be driven by feldspar type. The second principal component (PC2) has high positive loadings for Al, potassium feldspar, $^{87}Sr/^{86}Sr$, and plagioclase, and strong negative loadings for ε_{Nd}, calcite, Na, and Ca. Positive PC2 may be associated with a composition that is more clastic, while negative PC2 may be associated with more carbonate. The third principal component has high positive loadings for Ca, Fe, Mg, Na, and chlorite, and strong negative loadings for ε_{Nd}, kaolinite, and smectite. This dichotomy may be associated with mafic versus felsic compositions.

K-means cluster analysis was used to determine the appropriate grouping of the major element, isotope, and mineralogy PCA results. Catchment bed sediment was used for this analysis. To determine the appropriate number of sample groups, we applied the k-means cluster analysis with group numbers of 2-9, respectively, and assessed the silhouette values of each respective clustering result (Figure DR5). The clustering result with four groups has the greatest number of samples with high silhouette values; for example, there are 21 samples with silhouette values at or above 0.6, and 11 samples with silhouette values at or above 0.8 (Figure DR5). Therefore four groups is the most appropriate clustering solution for the catchment samples in combined major element, isotope, and mineralogy principal component space, and was used in this study (Figure DR6).

The groupings of samples contain some similarities to those identified in the major element PC space and the Sr-Nd isotope space. Samples collected from the Eastern Santa Clara River sub-catchment are again grouped together (L1, L2, L4, L5; Figure DR6), although sample L7 is also included in this group in the combined variable space. The Northern and Western SCR sub-catchment samples plot within the same group as the Southern Slopes samples, as also occurred in the isotope grouping (Figure 6). The Santa Rosa Island samples plot close together, but are separated from the other bed sediment samples, as also occurred in the isotope cluster analysis. Surprisingly, one group consists of samples L30, L24-1, GC, MC, and L3. This grouping did not occur in the isotopic or major element analyses. The SBB samples again plot within/near the expanded Southern Slopes group. Yet, in this combined major element, isotope, and mineralogy principal component space, the SBB Holocene flood samples and SBB LGM samples again have separation from one another, with the LGM samples again plotting closer to the SRI (Channel Island) samples.

Proportional suspended sediment flux to the Santa Barbara Bight

Warrick and Farnsworth (2009) calculated the mean annual suspended sediment fluxes of the Santa Clara River (SCR), Ventura River, Santa Ynez Mountains coastal creeks and Channel Islands creeks. As only the creeks north of the drainage divides on the Channel Islands contribute sediment to the Santa Barbara Bight, we used half the value of the Channel Islands creeks suspended sediment flux for our calculations. In Warrick and Mertes (2009), the mean annual suspended-sediment budget of watersheds within the SCR catchment is presented. We estimated the proportions of each creek watershed's mean annual suspended-sediment budget within the SCR, and assumed that these proportions also hold for the mean annual suspended sediment fluxes. Then we calculated the mean annual suspended sediment flux proportion of each source area (Eastern SCR, Northwest SCR as represented by the Northern SCR geographic region [Figure 2C], Western SCR, Southern Slopes and Channel Islands). We added together the Southern Slopes and Western SCR proportions to represent the extended Southern Slopes source area. The results of these calculations are presented in Table DR6.

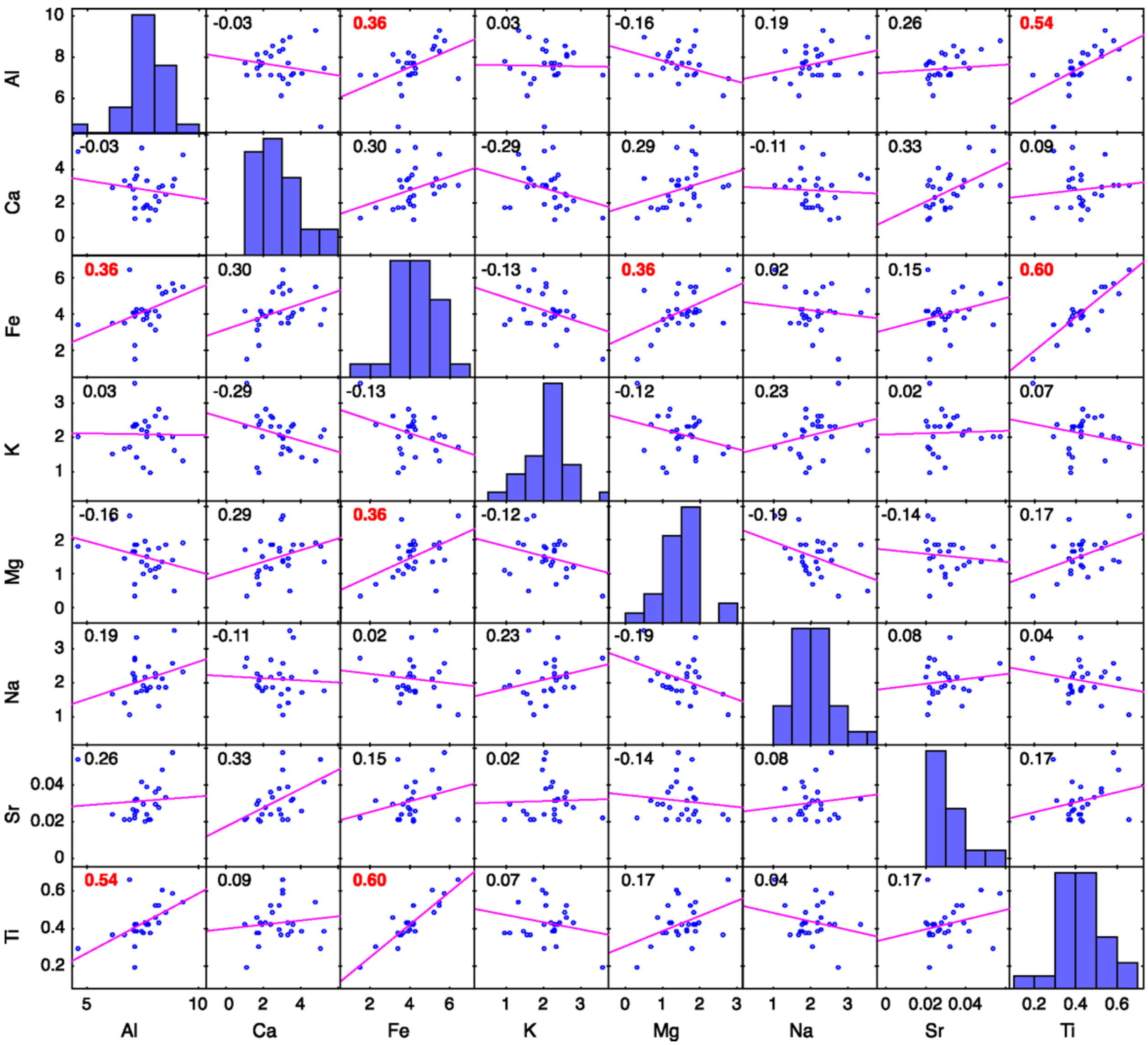

Figure DR1. Major element correlation matrix and elemental histograms. Correlation lines in pink. Kendall's rank correlation coefficients displayed in the top left of each correlation plot; red text indicated significant correlation. All stream bed sediment and sediment core samples (n=27) were used in correlation plots except for sample L4 in the Ti plots, L29 in the Na plots, and L2 and L4 in the Sr plots, as the respective elemental concentrations in those samples were greater than the 2□ range of all the samples (n=27).

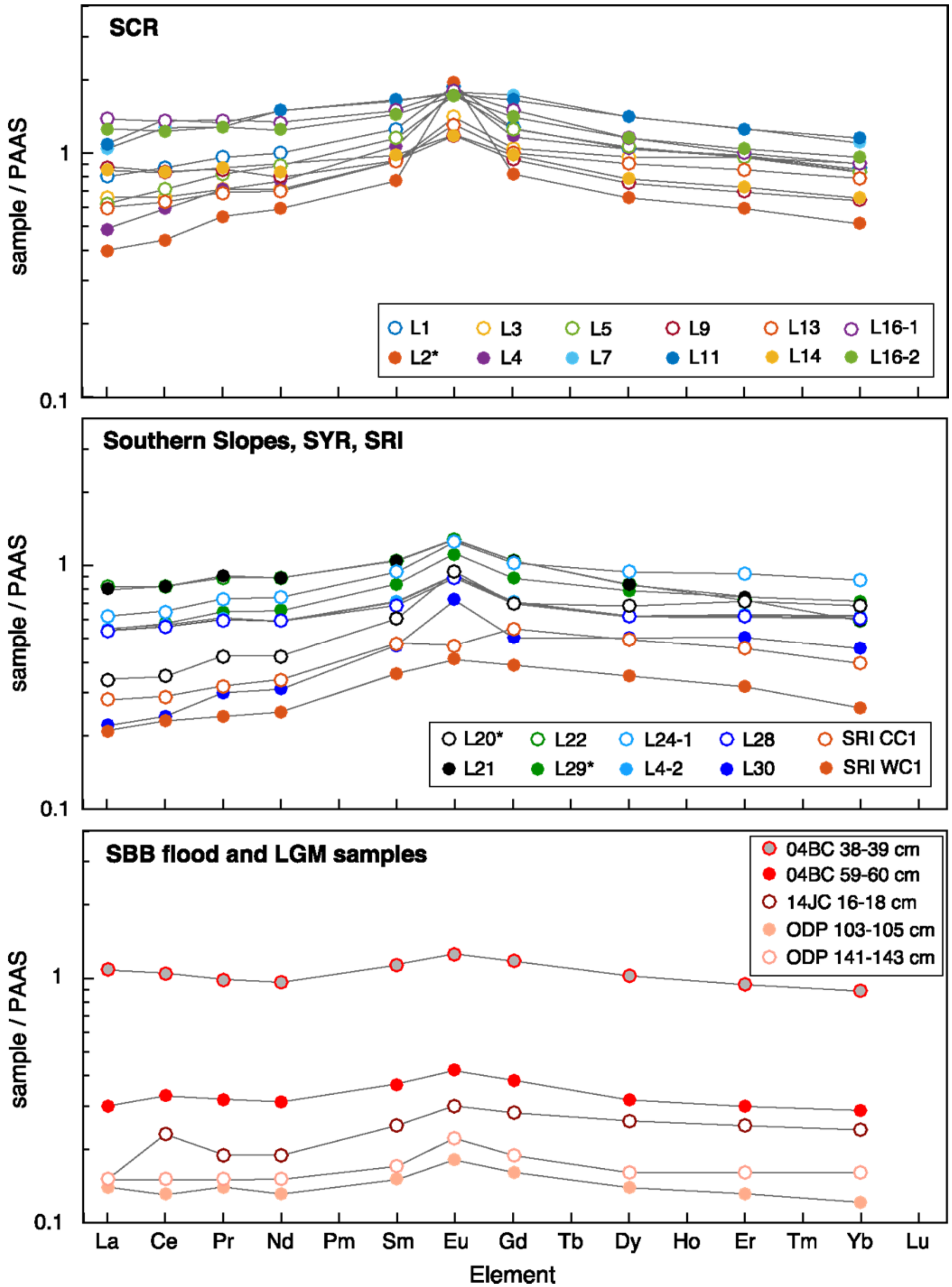

Figure DR2. Shale-normalized (PAAS; McLennan, 1989) REE patterns for stream bed sediment samples and sediment core samples. Asterisks denote averaging of results from multiple analyses of a sample. SCR–Santa Clara River catchment, VR–Ventura River catchment, SRI–Santa Rosa Island, SYR–Santa Ynez River catchment, SBB–Santa Barbara Basin, LGM–last glacial maximum.

Figure DR3. K-means clustering analysis of catchment samples major element PC1 and PC2. Clustering results in left panels and silhouette values for each clustering result in the corresponding right panels. The centroid of each k-means cluster is denoted by black 'X'.

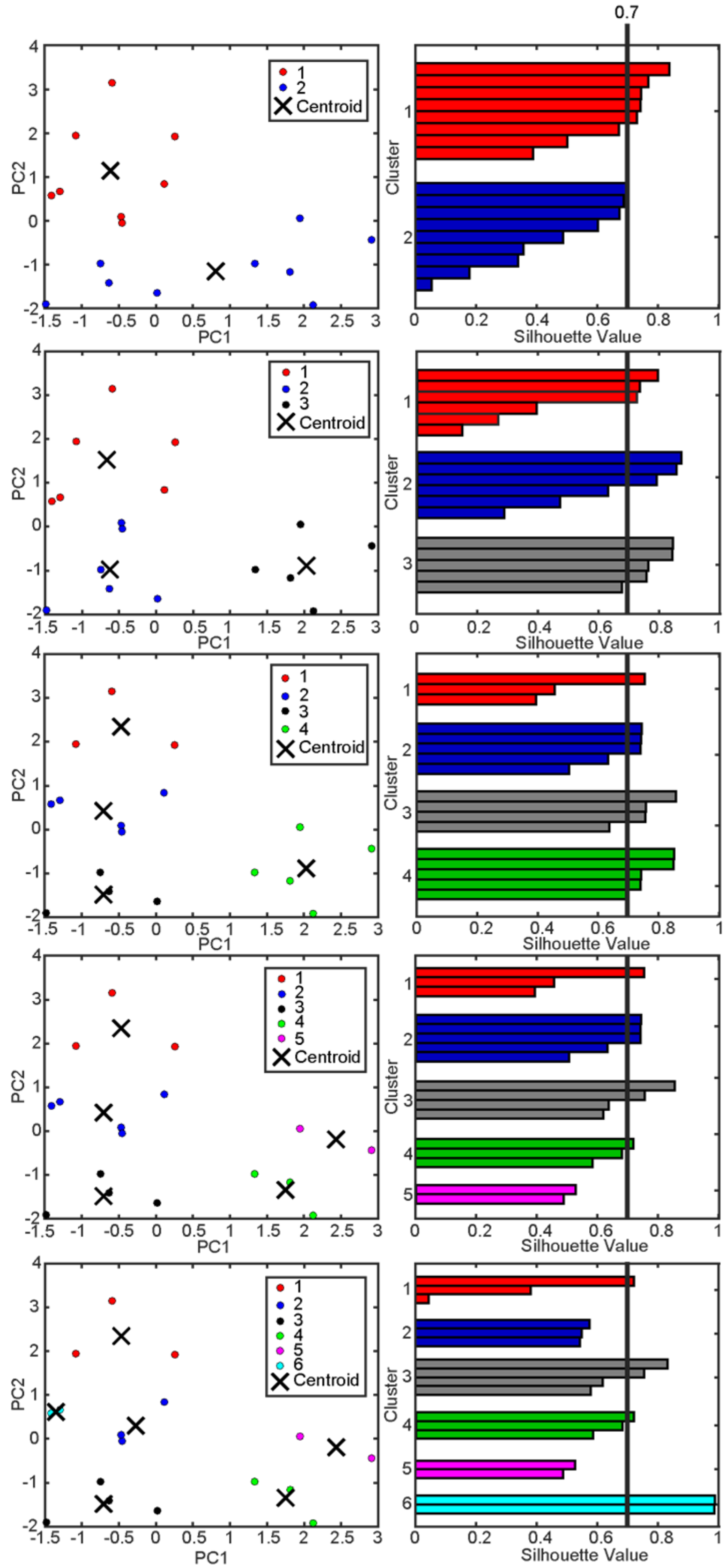

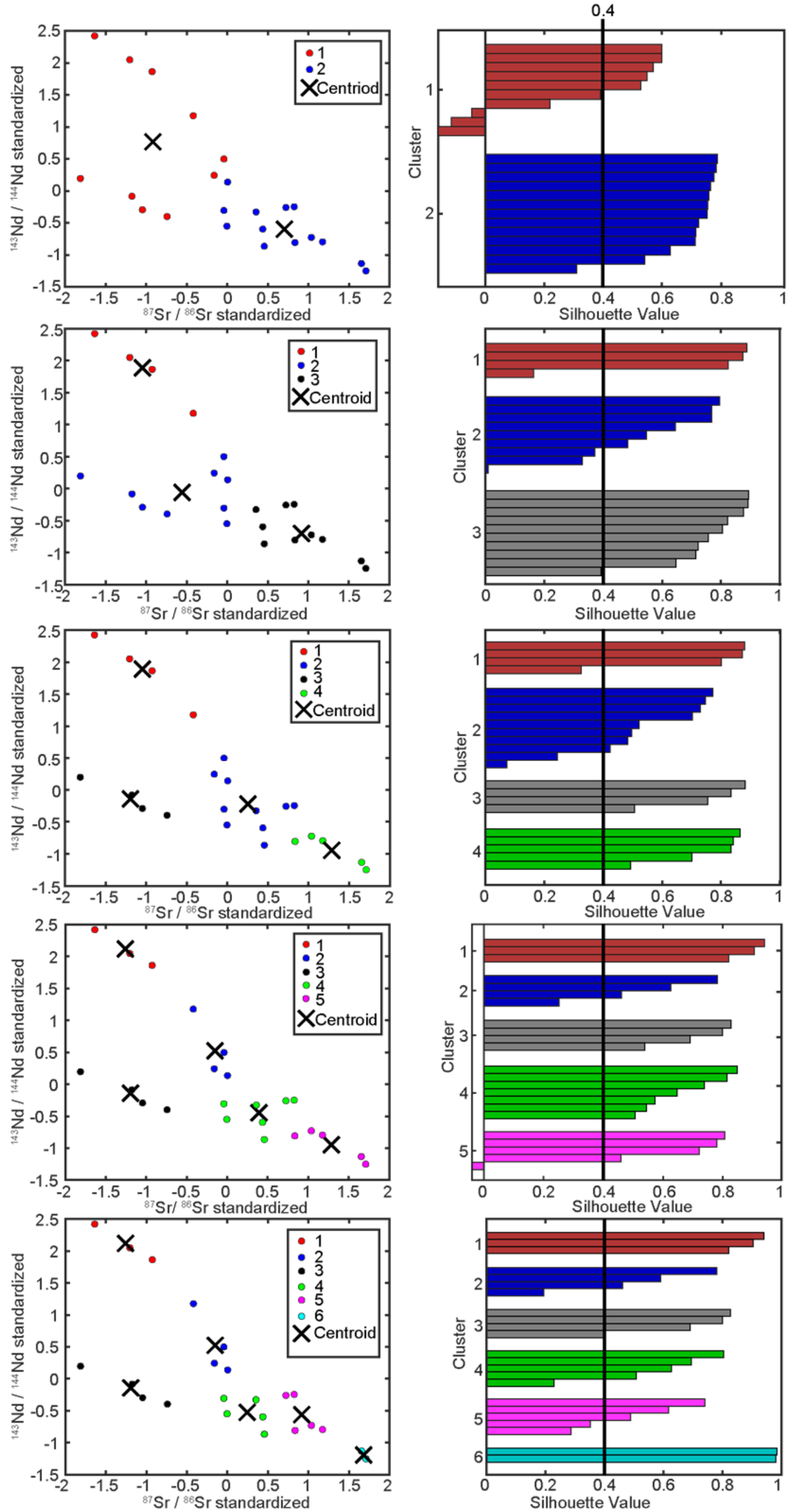

Figure DR4. K-means clustering analysis of catchment samples $^{87}Sr/^{86}Sr$ and $^{143}Nd/^{144}Nd$. Clustering results in left panels and silhouette values for each clustering result in the corresponding right panels. The centroid of each k-means cluster is denoted by black ‘X’.

Figure DR5. K-means clustering analysis silhouette profiles of catchment samples' major element compositions (Al, Ca, Fe, K, Mg, Na, Ti), $^{87}Sr/^{86}Sr$, ε_{Nd}, and predominant mineralogy (plagioclase, potassium feldspar, quartz, calcite, muscovite, illite, kaolinite, smectite, and chlorite). The colored profile (four clusters) is considered the most appropriate grouping, and was used for further analysis.

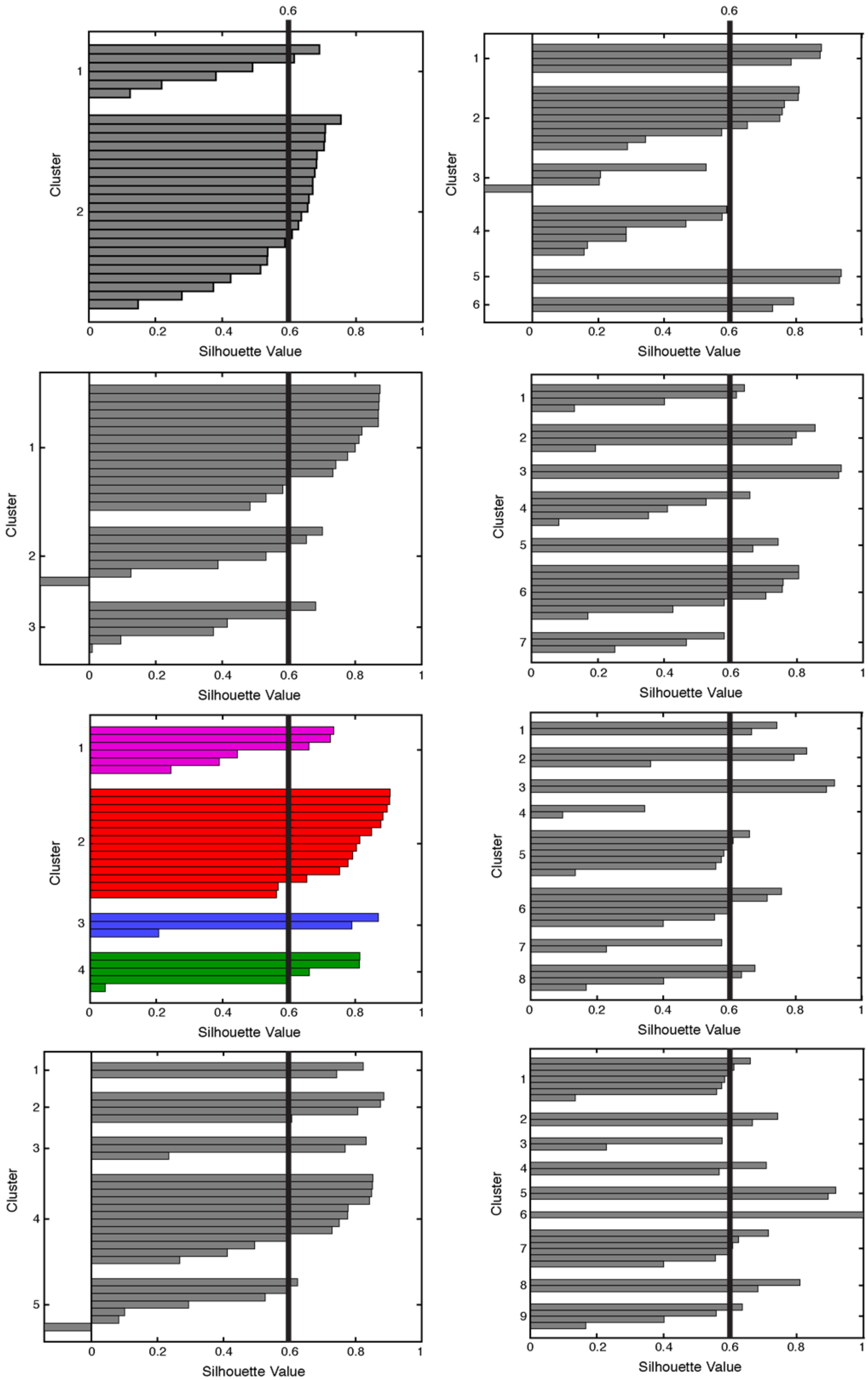

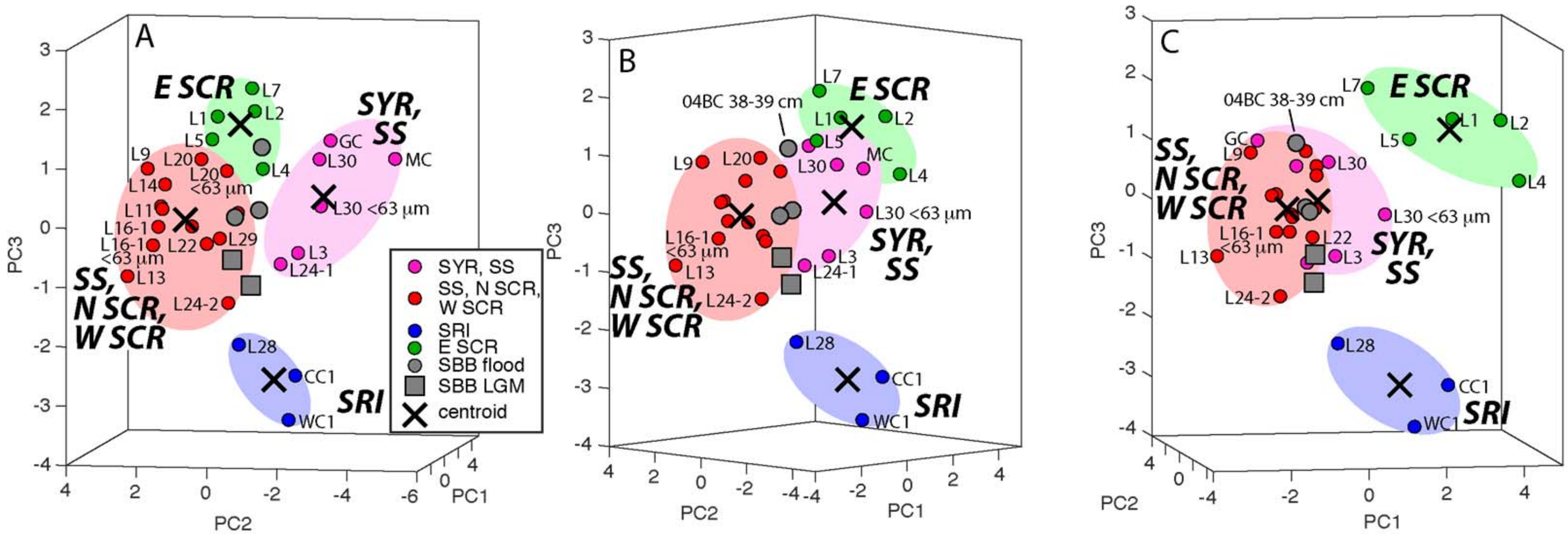

Figure DR6. Stream bed sediment and Santa Barbara Basin (SBB) sediment core samples expressed as the first (PC1), second (PC2), and third (PC3) principal components after combined principal component analysis of major element (Al, Ca, Fe, K, Mg, Na, Ti), $^{87}Sr/^{86}Sr$, ε_{Nd}, and predominant mineralogy (plagioclase, potassium feldspar, quartz, calcite, muscovite, illite, kaolinite, smectite, and chlorite) (Table DR6). Samples CC1 sand, WC1 sand, and the SBB samples were excluded from the PC analysis. The principal component scores were calculated for the SBB samples using the loadings in Table DR6. Composition groups identified by k-means cluster analysis of the stream bed sediment samples are shaded. The three panels (A, B, C) are views of the same plot rotated about a vertical axis. Composition group abbreviations: SYR–Santa Ynez River, SS–Southern Slopes, N SCR–Northern Santa Clara River, W SCR–Western Santa Clara River, SRI–Santa Rosa Island, E SCR–Eastern Santa Clara River, SBB–Santa Barbara Basin, LGM–Last Glacial Maximum.

TABLE DR1. SLIP RATE ESTIMATES FOR SELECTED FAULTS IN THE WESTERN TRANSVERSE RANGES, SOUTHERN CALIFORNIA, U.S.A.

Fault name	Slip rate (mm/yr)	Reference
Big Pine	2 – 7	Peterson and Wesnousky (1994), and therein
Hollywood	0.33 – 0.75	Peterson and Wesnousky (1994), and therein
Holser	0 – 0.4	Peterson (1996)
Malibu Coast	0.03 – 0.09	Peterson and Wesnousky (1994), and therein
Mission Ridge/Arroyo Parida	0.35 – 1.27	Rockwell et al. (1984)
Northridge	0.35 – 1.7	Davis and Namson (1994); Dolan et al. (1997); Huftile and Yeats (1996)
Oak Ridge	1.7 – 12.5	Huftile and Yeats (1996); Peterson and Wesnousky (1994), and therein
Raymond	0.10 – 0.22	Peterson and Wesnousky (1994), and therein
Red Mountain	0.31 – 7.16	Huftile and Yeats (1996)
San Andreas (Tejon and Cajon Passes)	16 – 38	Peterson and Wesnousky (1994), and therein
San Cayetano	0.85 – 10.7	Huftile and Yeats (1996); Peterson and Wesnousky (1994), and therein; Rockwell (1988);
San Gabriel	0.5 – 1	Peterson and Wesnousky (1994), and therein
Santa Cruz Island	0.2 – 0.9	Wesnousky (1986), and therein
Santa Monica	0.27 – 5.9	Davis and Namson (1994); Dolan and Pratt (1997); Peterson and Wesnousky (1994), and therein
Santa Rosa Island	1	Colson thesis, 1996
Santa Susana	2.1 – 9.8	Huftile and Yeats (1996)
Santa Ynez	0.05 – 6.7	Peterson and Wesnousky (1994), and therein
Sierra Madre	0.36 – 5.0	Peterson and Wesnousky (1994), and therein; Tucker and Dolan (2001); Rubin et al. (1998)
Simi	0.4 – 0.9	Gonzalez and Rockwell (1991); Hitchcock (2001)
Ventura	0.8 – 2.4	Peterson and Wesnousky (1994)

TABLE DR2. DESCRIPTION OF SAMPLE LOCATIONS IN SOUTHERN CALIFORNIA.

Sample	Location		Stream name	Sample type	Sampling notes
	*Lat (ºN)	*Long (ºW)			
Santa Clara River					
2	34.429028	118.354694	Santa Clara River	bed sediment	†N.D.
3	34.553722	118.414778	Bouquet Creek	bed sediment	N.D.
4	34.424028	118.483056	Santa Clara River	bed sediment	Grain size ranges from clay to 50 cm in diameter. Bedload contains fragments of (sub-rounded) gneiss, white and pink granite, basalt, chlorite, phyllite, tuff, sandstone grading into phyllite.
5	34.425972	118.579361	Santa Clara River	bed sediment	Grain size ranges same as Loc. 4. Rock fragments same as Loc. 4 plus sandstone.
7	34.418222	118.657250	N.D.	bed sediment	SCR tributary-Chiquito Canyon. Bedload clases up to 40 cm in length; up to 300 cm near bridge. Gneiss, granite, sandstone.
9	34.616833	118.745139	Piru Creek	bed sediment	Boulders in streambed up to 1 m in length. Rocks in steambed: gneiss, sandstone, granite.
11	34.703972	118.939583	Piru Creek	bed sediment	Many boulders in creek (>1 m in length). Granite and gneiss.
13	34.394639	118.799361	Santa Clara River	bed sediment	Grain size ranges from clay/silt up to boulders 1 m in length. Rock types: Granite, gneiss, conglomerate, sandstone. Well-rounded to sub-rounded.
14	34.444528	118.927028	Sespe Creek	bed sediment	Grain size ranges from clay/silt up to 1.5 m boulders. Gneiss, andesite, red sandstone (Sespe Fm.), tan sandstone, granite, red conglomerate. Rounded to sub-angular.
16	34.356139	119.035056	Santa Clara River	bed sediment	Sandstone, gneiss, granite. Clast size clay/silt up to 40 cm.
Ventura River					
20	34.424444	119.302278	Coyote Creek	bed sediment	Bedload sample collected just above weir. Clasts are sub-rounded to rounded; range in size from silt/sand to 70 cm. Sandstones, chert, granite/diorite, limestone/diatomite.
21	34.418278	119.825944	Ventura River	bed sediment	Clasts sub-angular to well-rounded. Grain size is sand up to boulders ~ <2 m in length. Sandstones, granite, conglomerate, breccia. All boulders are sandstone.
Santa Ynez Mountains					
22	34.545472	119.791694	Goleta Slough	bed sediment	N.D.

29	34.669750	120.445306	Gaviota Creek	bed sediment	Gaviota Beach. Possible influence of SB littoral cell. Mouth of creek closed-off from ocean. Sandstone, chert.
GC	N.D.	N.D.	Gaviota Creek	suspended load	N.D.
MC	34.412583	119.687500	Mission Creek	suspended load	N.D.
Santa Ynez River					
24	34.545472	119.791694	Santa Ynez River	bed sediment	Bedload samples collected above and below weir; also collected bedload mud. Clasts in bedload range from mud to ~1 m. Rocks: diatomite/limestone, chert, sandstone, serpentinite, greenstone.
28	34.471361	120.226806	Santa Ynez River	bed sediment	Grain size: sand. Rounded to sub-rounded. Rocks: sandstone, diatomite, limestone (fossiliferous), granite, tuff, greenstone, serpentinite, chert, siltstone.
30	34.677917	120.424944	Santa Ynez River	bed sediment	Clasts range from clay/mud to ~200 mm. Well-rounded to sub-angular. Sandstone, diatomite, chert, greenstone (few), serpentinite (few).
Santa Rosa Island					
WC1	33.989500	120.048600	N.D.	bed sediment	Water Canyon
WC2	33.993233	120.040800	N.D.	bed sediment	Water Canyon
CC1	34.007800	120.050967	N.D.	bed sediment	Cherry Canyon
CC2	34.008717	120.050150	N.D.	bed sediment	Cherry Canyon

[*]WGS84 projection.

[†]No data.

TABLE DR3. MAJOR, MINOR, AND TRACE ELEMENT ANALYTICAL RESULTS FOR LABORATORY STANDARDS GBM908-10 AND MRGEO08.

Standard sample batch	Al (%)	Ca (%)	Fe (%)	Ga (ppm)	In (ppm)	K (%)	Mg (%)	Na (%)	Nb (ppm)	Rb (ppm)	Sr (ppm)	Ta (ppm)	Ti (%)	Y (ppm)	Rb/Sr
GBM908-10 Target Range															
Lower bound	6.40	3.33	5.21	18.65	0.064	1.86	1.59	2.02	9.3	153.0	258	0.68	0.591	36.2	
Upper bound	7.84	4.10	6.39	22.90	0.092	2.29	1.97	2.50	11.6	187.0	316	0.97	0.733	44.5	
SPR0901-04BC sample batch															
GBM908-10	7.08	4.01	5.71	20.40	0.081	2.14	1.91	2.18	10.9	174.0	297	0.82	0.673	39.1	0.59
GBM908-10	7.23	3.84	5.62	21.00	0.069	2.26	1.88	2.26	11.1	186.0	303	0.82	0.684	41.8	0.61
GBM908-10	7.19	3.89	5.65	21.40	0.086	2.10	1.87	2.19	10.7	176.5	301	0.75	0.666	39.9	0.59
GBM908-10	7.16	3.73	5.45	20.30	0.080	2.02	1.80	2.12	10.3	177.5	290	0.75	0.650	37.9	0.61
GBM908-10	7.39	4.01	5.84	21.40	0.067	2.22	1.89	2.30	10.3	181.5	304	0.78	0.697	41.0	0.60
GBM908-10	7.01	3.78	5.56	19.60	0.073	2.13	1.79	2.20	9.9	160.0	291	0.72	0.648	37.9	0.55
standard deviation	0.13	0.12	0.13	0.71	0.007	0.09	0.05	0.06	0.4	8.9	6	0.04	0.019	1.6	0.02
standard error	0.05	0.05	0.05	0.29	0.003	0.04	0.02	0.03	0.2	3.6	2	0.02	0.008	0.7	0.01
MV0811-14JC sample batch															
GBM908-10	6.98	3.64	5.40	20.7	0.074	2.07	1.78	2.11	10.1	166.0	294	0.75	0.638	37.7	0.56
GBM908-10	6.97	3.75	5.53	20.6	0.077	2.10	1.84	2.14	10.4	173.0	293	0.73	0.659	39.1	0.59
GBM908-10	6.97	3.73	5.51	20.8	0.074	2.08	1.85	2.15	10.0	163.0	297	0.71	0.667	35.4	0.55
standard deviation	0.01	0.06	0.07	0.1	0.002	0.02	0.04	0.02	0.2	5.1	2	0.02	0.015	1.9	0.02
standard error	0.00	0.03	0.04	0.1	0.001	0.01	0.02	0.01	0.1	3.0	1	0.01	0.009	1.1	0.01
MRGeo08 Target Range															
Lower bound	7.00	2.35	3.61	17.50	0.161	2.79	1.24	1.76	19.3	187.0	272	1.48	0.454	24.3	
Upper bound	8.57	2.90	4.43	21.50	0.207	3.43	1.54	2.18	23.8	229.0	332	1.92	0.566	29.9	
SPR0901-04BC sample batch															
MRGeo08	7.57	2.71	3.88	18.75	0.178	3.13	1.34	1.96	20.9	211.0	308	1.49	0.497	27.8	0.69
MRGeo08	7.35	2.72	4.00	18.25	0.168	3.10	1.34	1.97	20.5	199.5	308	1.49	0.493	27.0	0.65
MRGeo08	7.63	2.80	4.24	19.40	0.171	3.31	1.37	2.11	22.8	189.0	318	1.52	0.526	27.0	0.59
MRGeo08	7.33	2.71	4.00	18.90	0.172	3.20	1.32	2.08	22.1	191.5	326	1.55	0.512	27.8	0.59
MRGeo08	6.67	2.42	3.60	18.35	0.171	2.84	1.19	1.85	20.5	172.0	285	1.60	0.457	23.9	0.60

MRGeo08	7.63	2.81	4.15	18.95	0.159	3.31	1.40	2.10	21.1	186.0	325	1.64	0.53	27.2	0.57
MRGeo08	7.68	2.67	3.98	18.70	0.173	3.19	1.36	2.03	22.6	208.0	315	1.52	0.502	29.0	0.66
MRGeo08	7.48	2.67	4.01	18.25	0.174	3.18	1.32	2.03	22.0	192.5	311	1.52	0.489	27.0	0.62
standard deviation	0.33	0.12	0.19	0.40	0.006	0.15	0.06	0.09	0.9	12.5	13	0.05	0.023	1.5	0.04
standard error	0.12	0.04	0.07	0.14	0.002	0.05	0.02	0.03	0.3	4.4	5	0.02	0.008	0.5	0.01
MV0811-14JC sample batch															
MRGeo08	7.00	2.57	3.87	19.05	0.175	3.04	1.29	2.00	20.7	175.5	310	1.44	0.499	26.0	0.57
MRGeo08	7.25	2.55	3.80	18.30	0.180	3.03	1.29	1.93	21.6	199.5	304	1.53	0.492	27.9	0.66
MRGeo08	7.51	2.52	3.89	18.70	0.174	3.11	1.32	1.91	19.7	197.0	307	1.48	0.472	26.3	0.64
standard deviation	0.26	0.03	0.05	0.38	0.003	0.04	0.02	0.05	1.0	13.2	3	0.05	0.014	1.0	0.05
standard error	0.15	0.01	0.03	0.22	0.002	0.03	0.01	0.03	0.5	7.6	2	0.03	0.008	0.6	0.03
Stream bed sediment and ODP 893A glacial sample batch															
MRGeo08	7.52	2.70	4.03	20.30	0.189	3.28	1.34	2.04	22.0	200.0	311	1.68	0.515	26.7	0.64
MRGeo08	7.15	2.62	3.92	19.65	0.180	3.21	1.28	2.00	21.3	184.0	303	1.59	0.497	25.5	0.61
standard deviation	0.26	0.06	0.08	0.46	0.006	0.05	0.04	0.03	0.5	11.3	6	0.06	0.013	0.8	0.03
standard error	0.19	0.04	0.06	0.33	0.005	0.03	0.03	0.02	0.4	8.0	4	0.04	0.009	0.6	0.02

TABLE DR4. RARE EARTH ELEMENT ANALYTICAL RESULTS FOR INTERNAL LABORATORY STANDARDS JA-1 AND BCR-2

Element	JA-1				BCR-2		
	GeoRem preferred values	Aliquot 1	Aliquot 2	Error (%)	GeoRem preferred values	Aliquot 1	Error (%)
La (ppm)	4.88 ± 0.13	4.9 ± 0.1	4.8 ± 0.1	0.9	25.08 ± 0.2	24.5 ± 0.6	2.4
Ce (ppm)	13.15 ± 0.58	13.2 ± 0.3	13.0 ± 0.4	0.7	53.12 ± 0.3	54.02 ± 1.3	1.7
Pr (ppm)	2.082 ± 0.054	2.0 ± 0.1	2.0 ± 0.1	1.4	6.827 ± 0.044	6.7 ± 0.2	1.9
Nd (ppm)	10.69 ± 0.29	10.6 ± 0.2	10.4 ± 0.3	1.8	28.26 ± 0.37	28.3 ± 0.7	0.0
Sm (ppm)	3.396 ± 0.077	3.4 ± 0.3	3.3 ± 0.2	0.8	6.547 ± 0.047	6.5 ± 0.3	0.1
Eu (ppm)	1.112 ± 0.027	1.1 ± 0.1	1.1 ±0.1	0.0	1.989 ± 0.024	2.0 ± 0.1	1.5
Gd (ppm)	4.15 ± 0.12	4.1 ± 0.2	4.0 ± 0.2	2.1	6.811 ± 0.08	6.5 ± 0.3	4.1
Dy (ppm)	4.75 ± 0.11	4.7 ± 0.2	4.7 ± 0.1	1.0	6.424 ± 0.055	6.4 ± 0.3	0.0
Er (ppm)	2.959 ± 0.065	3.0 ± 0.1	3.0 ± 0.2	0.1	3.67 ± 0.04	3.7 ± 0.1	0.4
Yb (ppm)	2.949 ± 0.085	3.0 ± 0.1	2.9 ± 0.1	0.9	3.392 ± 0.036	3.4 ± 0.2	0.5

TABLE DR5. PRINCIPAL COMPONENT ANALYSIS LOADINGS OF MAJOR ELEMENT, $^{87}Sr/^{86}Sr$, ε_{Nd}, AND MINERALOGY COMBINED ANALYSIS.

Variable	Loading		
	PC1	PC2	PC3
Al	**0.31**	**0.41**	0.01
Ca	0.05	**-0.26**	**0.47**
Fe	**0.27**	**0.07**	**0.42**
K	**-0.29**	**0.32**	**0.18**
Mg	-0.04	**-0.20**	**0.29**
Na	**-0.11**	**-0.32**	**0.24**
Ti	**0.29**	**0.09**	**0.19**
$^{87}Sr/^{86}Sr$	**-0.40**	**0.23**	-0.03
ε_{Nd}	**0.34**	**-0.34**	**-0.34**
Plagioclase	**0.43**	**0.22**	**0.12**
Potassium feldspar	**-0.25**	**0.33**	**0.10**
Quartz	**-0.28**	-0.04	**0.07**
Calcite	**-0.16**	**-0.33**	**0.07**
Muscovite	0.01	0.00	**0.19**
Illite	**-0.10**	**-0.17**	0.03
Kaolinite	0.05	**-0.10**	**-0.32**
Smectite	**-0.08**	**-0.10**	**-0.22**
Chlorite	-0.01	**-0.15**	**0.21**
Variance	28%	26%	13%

Note: Bolded values indicate that a variable has a higher loading than would be expected if each variable were independent of one another. Loadings were bolded if their value was greater than the square root of (1/n), where n = the number of elements used in the principal component analysis.

TABLE DR6. STRONTIUM AND NEODYMIUM ISOTOPIC RESULTS FROM SOURCE LOCALITIES WITHIN THE STUDY AREA (SOUTHERN CALIFORNIA).

Locality	Rock type	$^{*87}Sr/^{86}Sr_{(0)}$	$^{143}Nd/^{144}Nd_{(0)}$	$^{\dagger}\varepsilon_{Nd(0)}$	Reference
Mendenhall Gneiss	mafic granulites	0.70717	-	-	Barth et al. (1995)
Mendenhall Gneiss	mafic granulites	0.70569	-	-	Barth et al. (1995)
Mendenhall Gneiss	mafic granulites	0.70779	-	-	Barth et al. (1995)
Mendenhall Gneiss	mafic granulites	0.71587	-	-	Barth et al. (1995)
Mendenhall Gneiss	mafic granulites	0.70618	-	-	Barth et al. (1995)
Mendenhall Gneiss	mafic granulites	0.70466	-	-	Barth et al. (1995)
Mendenhall Gneiss	mafic granulites	0.70567	-	-	Barth et al. (1995)
Mendenhall Gneiss	mafic granulites	0.70827	-	-	Barth et al. (1995)
Mendenhall Gneiss	augen gneiss	0.71815	-	-	Barth et al. (1995)
Mendenhall Gneiss	augen gneiss	0.70943	-	-	Barth et al. (1995)
Mendenhall Gneiss	felsic gneiss	0.70892	-	-	Barth et al. (1995)
Mendenhall Gneiss	felsic gneiss	0.71088	-	-	Barth et al. (1995)
Mendenhall Gneiss	felsic gneiss	0.73774	-	-	Barth et al. (1995)
Mendenhall Gneiss	felsic gneiss	0.7248	-	-	Barth et al. (1995)
Mendenhall Gneiss	felsic gneiss	0.70694	-	-	Barth et al. (1995)
Mendenhall Gneiss	felsic gneiss	0.75602	-	-	Barth et al. (1995)
Mendenhall Gneiss	aluminous gneiss	0.74607	-	-	Barth et al. (1995)
Mendenhall Gneiss	aluminous gneiss	0.74636	-	-	Barth et al. (1995)
Bouquet Reservoir	gneiss	0.7099	-	-	Kistler et al. (1973)
Liebre Mountain	granitic	0.7095	-	-	Kistler et al. (1973)
Mt. Pinos	gneiss	0.7168	-	-	Kistler et al. (1973)
Mt. Pinos	-	0.7092	-	-	Kistler et al. (1973)
Mt. Pinos	-	0.7136	-	-	Kistler et al. (1973)
Mt. Pinos	amphibolite		0.511735	-17.6	Bennett and DePaolo (1987)
Mt. Pinos	pelitic schist		0.510731	-37.2	Bennett and DePaolo (1987)
Mt. Pinos	augen gneiss		0.51083	-35.3	Bennett and DePaolo (1987)
Tranquillon volcanics	rhyolite	0.710617	0.512738	2.0	Cole and Basu (1995)
Tranquillon volcanics	rhyolite	0.710729	0.512727	1.7	Cole and Basu (1995)
Tranquillon volcanics	rhyolite	0.712017	0.512759	2.4	Cole and Basu (1995)
Tranquillon volcanics	basaltic andesite	0.704033	0.512867	4.5	Cole and Basu (1995)
Tranquillon volcanics	basaltic andesite	0.704125	0.512943	5.9	Cole and Basu (1995)
Santa Cruz Island, [§]WPC	whole rock	0.70372	-	-	Hammond Gordon and Weigland (2004)
Santa Cruz Island, WPC	whole rock	0.70357	-	-	Hammond Gordon and Weigland (2004)
Santa Cruz Island, WPC	whole rock	0.7037	-	-	Hammond Gordon and Weigland (2004)
Santa Cruz Island, WPC	whole rock	0.70343	-	-	Hammond Gordon and Weigland (2004)
Santa Cruz Island, WPC	whole rock	0.70367	-	-	Hammond Gordon and Weigland (2004)
Santa Cruz Island, WPC	whole rock	0.70352	-	-	Hammond Gordon and Weigland (2004)
Sediment core [#]ODP 893A	silicate [**]>63 µm	-	0.512038	-11.7	Murphy and Thomas (2010)
Sediment core ODP 893A	silicate >63 µm	-	0.512027	-11.9	Murphy and Thomas (2010)
Sediment core ODP 893A	silicate >63 µm	-	0.512024	-12.0	Murphy and Thomas (2010)
Sediment core ODP 893A	silicate >63 µm	-	0.512032	-11.8	Murphy and Thomas (2010)

Note: Dashes indicate data not determined.

[*]Subscript (0) denotes present-day measurement.

$^{\dagger 143}Nd/^{144}Nd_{CHUR} = 0.512638$

[§]WPC = Willows Plutonic Complex.

[#]Ocean Drilling Program.

[**]Greater than 63 µm size fraction.

TABLE DR7. CALCULATION OF SEDIMENT FLUX TO SANTA BARBARA BIGHT PROPORTIONS (SOUTHERN CALIFORNIA, U.S.A.)

River or region	*Mean annual suspended sediment flux to Santa Barbara Bight (t/yr)	Mean annual suspended sediment flux to Santa Barbara Bight proportion
Santa Ynez Mountain coastal creeks	640000	0.15
Ventura River	270000	0.06
Santa Clara River	3100000	0.72
Channel Island creeks, northern drainages	295,000	0.07
Total:	4305000	1.00

Santa Clara River catchment	Sub-catchment	†Approximate mean annual suspended sediment budget (Mt/yr)
Castaic Creek	North SCR	0.55
SCR at LA co line	Eastern SCR	0.9
Piru Creek	North SCR	0.8
Hopper Creek	Western SCR	0.15
Sespe Creek	Western SCR	1.25
SCR at Montalvo + Santa Paula Creek	Western SCR	3.5
Total:		7.15

Santa Clara River catchment	Mean annual suspended sediment budget proportion	Mean annual suspended sediment flux to Santa Barbara Bight proportion
Eastern SCR	0.13	0.09
Northern SCR	0.19	0.14
Western SCR	0.69	0.49
Total:	1.00	0.72

Source Areas	Mean annual suspended sediment flux to Santa Barbara Bight proportion
Extended Southern Slopes	0.70
Eastern SCR	0.09
Northern SCR	0.14
Channel Islands (SRI)	0.07
Total	1.00

*From Warrick and Farnsworth (2009).

†From Warrick and Mertes (2009:Figure 10A).

References Cited

Barth, A. P., Wooden, J. L., Tosda, R. M., Morrison, J., Dawson, D. L., and Hernly, B. M., 1995, Origin of gneisses in the aureole of the San Gabriel anorthosite complex and implications for the Proterozoic crustal evolution of southern California: Tectonics, v. 14, no. 3, p. 736.

Bennett, V. C., and DePaolo, D. J., 1987, Proterozoic crustal history of the western United States as determined by neodymium isotopic mapping: Geological Society of America Bulletin, v. 99, no. 5, p. 674-685.

Cole, R. B., and Basu, A. R., 1995, Nd-Sr isotopic geochemistry and tectonics of ridge subduction and middle Cenozoic volcanism in western California: Geological Society of America Bulletin, v. 107, no. 2, p. 167-179.

Colson, K., 1996, Neotectonics of the left-lateral Santa Rosa Island Fault, Western Transverse Ranges, Southern California [Master of Science: San Diego State Univesity, 110 p.

Davis, T. L., and Namson, J. S., 1994, A balanced cross-section of the 1994 Northridge earthquake, southern California: Nature, v. 372, no. 6502, p. 167.

Dolan, J. F., and Pratt, T. L., 1997, High‐resolution seismic reflection profiling of the Santa Monica Fault Zone, west Los Angeles, California: Geophysical Research Letters, v. 24, no. 16, p. 2051.

Dolan, J. F., Sieh, K., Rockwell, T. K., Guptill, P., and Miller, G., 1997, Active tectonics, paleoseismology, and seismic hazards of the Hollywood fault, northern Los Angeles basin, California: Geological Society of America Bulletin, v. 109, no. 12, p. 1595-1616.

Gonzalez, T., and Rockwell, T. K., 1991, Holocene activity of the Springville Fault in Camarillo, Transverse Ranges, Southern California; Preliminary observations, *in* Blake, T. F., and

Larson, R. A., eds., Engineering Geology along the Simi-Santa Rose Fault System and Adjacent Areas, Simi Valley to Camarillo, Ventura County, California; Field Trip Guidebook of the 1991 Annual Field Trip, Association of Engineering Geologists, Southern California Section, p. 369-383.

Hammond Gordon, J., and Weigland, P. W., A slice of immature arc rocks marooned on Santa Cruz Island, California, *in* Proceedings The Fourth California Islands Symposium: Update on the Status of Resources1994, Santa Barbara Museum of Natural History, p. 235-243.

Huftile, G. J., and Yeats, R. S., 1996, Deformation rates across the placerita (Northridge M(w)=6.7 aftershock zone) and Hopper Canyon segments of the western transverse ranges deformation belt: Bulletin of the Seismological Society of America, v. 86, no. 1, p. S3.

Kistler, R. W., Peterman, Z. E., Ross, D. C., and Gottfried, D., Strontium isotopes and the San Andreas Fault, *in* Proceedings Conference on Tectonic Problems of the San Andreas Fault System, Stanford University, 1973 1973, Volume XIII, Stanford University, p. 339-347.

McLennan, S. M., 1989, Rare earth elements in sedimentary rocks; influence of provenance and sedimentary processes: Reviews in Mineralogy and Geochemistry, v. 21, no. 1, p. 169-200.

Murphy, D. P., and Thomas, D. J., 2010, The negligible role of intermediate water circulation in stadial–interstadial oxygenation variations along the southern California margin: Evidence from Nd isotopes: Quaternary Science Reviews, v. 29, no. 19–20, p. 2442-2450.

Petersen, M. D., 1996, Probabilistic seismic hazard assessment for the state of California.

Petersen, M. D., and Wesnousky, S. G., 1994, Fault slip rates and earthquake histories for active faults in southern California: Bulletin of the Seismological Society of America, v. 84, no. 5, p. 1608.

Rockwell, T., 1988, Neotectonics of the San Cayetano fault, Transverse Ranges, California: GSA Bulletin, v. 100, no. 4, p. 500.

Rockwell, T. K., Keller, E. A., Clark, M. N., and Johnson, D. L., 1984, Chronology and rates of faulting of Ventura River terraces, California: Bulletin of the Geological Society of America, v. 95, no. 12, p. 1466.

Rubin, C. M., Lindvall, S. C., and Rockwell, T. K., 1998, Evidence for Large Earthquakes in Metropolitan Los Angeles: Science, v. 281, no. 5375, p. 398.

Tucker, A. Z., and Dolan, J. F., 2001, Paleoseismologic Evidence for a >8 Ka Age of the Most Recent Surface Rupture on the Eastern Sierra Madre Fault, Northern Los Angeles Metropolitan Region, California: Bulletin of the Seismological Society of America, v. 91, no. 2, p. 232.

Warrick, J. A., and Farnsworth, K. L., 2009, Sources of sediment to the coastal waters of the Southern California Bight: Geological Society of America Special Papers, v. 454, p. 39-52.

Warrick, J. A., and Mertes, L. A. K., 2009, Sediment yield from the tectonically active semiarid Western Transverse Ranges of California: Geological Society of America Bulletin, v. 121, no. 7-8, p. 1054-1070.

Wesnousky, S. G., 1986, Earthquakes, quaternary faults, and seismic hazard in California: Journal of Geophysical Research: Solid Earth, v. 91, no. B12, p. 12587-12631.